SUPPLEMENTARY INFORMATION
https://doi.org/10.1038/s41594-018-0132-7

nature structural & molecular biology

In the format provided by the authors and unedited.

NMD-degradome sequencing reveals ribosome-bound intermediates with 3′-end non-templated nucleotides

Tatsuaki Kurosaki[1,2], Keita Miyoshi[1,2,4], Jason R. Myers[3] and Lynne E. Maquat[1,2*]

[1]Department of Biochemistry and Biophysics, School of Medicine and Dentistry, University of Rochester, Rochester, NY, USA. [2]Center for RNA Biology, University of Rochester, Rochester, NY, USA. [3]Genomics Research Center, University of Rochester, Rochester, NY, USA. [4]Present address: Division of Invertebrate Genetics, National Institute of Genetics, Mishima, Shizuoka, Japan. *e-mail: lynne_maquat@urmc.rochester.edu

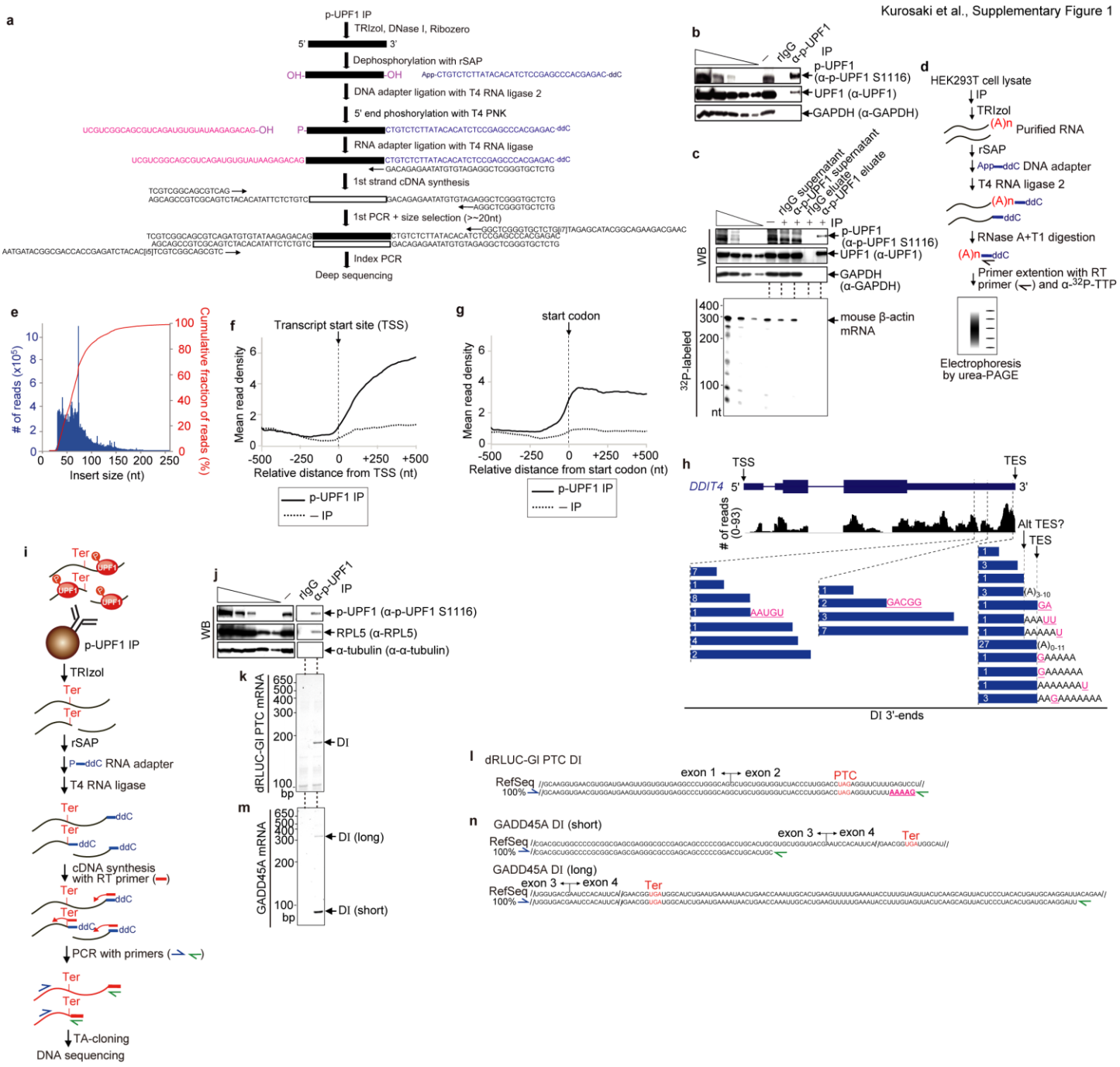

Supplementary Figure 1

Transcriptome-wide NMD-Degradome Sequencing (NMD-DegSeq) maps decay intermediate (DI) 3' ends, revealing the existence of not only homogeneous but also heterogeneous nontemplated nucleotide additions.

a, Supplemental details of transcriptome-wide NMD-DegSeq library construction. **b**, Western blot prior to (–) or after IP using rIgG or anti(α)-p-UPF1. The leftmost five lanes represent threefold serial dilutions of lysate prior to IP. **c**, Control experiment showing that there was neither RNA degradation during p-UPF1 immunoprecipitation (IP) nor nonspecific binding for anti(α)-p-UPF1 antibody using in vitro–synthesized and ^{32}P-labeled mouse β-actin mRNA, which is not an NMD target and was added to lysates prior to p-UPF1 IP. **d**, Primer extension assay workflow. See the Methods for experimental procedures. **e**, Size distribution (blue histogram) and cumulative size distribution (red line) of p-UPF1-bound DIs analyzed for NMD-DegSeq. **f**, Mean read density of exonic sequence reads ± 500 nucleotides (nt) relative to the transcription start site (TSS). Sequence reads from paired-end reads before (–) IP (dotted line) or after (solid line) p-UPF1 IP are shown. **g**, As in **f**, except for exonic sequence reads ± 500 nt relative to the translational start codon. **h**, As in

Fig. 1h, but for DDIT4 mRNA, aligned to the coding strand of the DDIT4 gene. TSS, transcription start site; TES, transcription end site; Alt TES, alternative transcription end site. **i**, Scheme for streamlined NMD-DegSeq. See the Methods for details. **j**, Western blotting (WB) before (−) or after IP of lysates of HEK293T-cells, which were treated with okadaic acid prior to lysis, using anti(α) p-UPF1 or, as a negative control, rabbit (r)IgG. The five leftmost lanes represent threefold serial dilutions of lysate prior to IP. **k**, SYBR Gold staining of the dRLUC-Gl PTC DI. **l**, Sequences of dRLUC-Gl PTC DIs in streamlined NMD-DegSeq. The PTC (red) and exon 1–exon 2 junction are shown in the reference sequence (RefSeq). PCR primers (sense, blue arrows; antisense, green arrows) and nontemplated nucleotide additions (pink) are provided in the DIs, for which numbers to the left of blue arrows denote the percent (%) that each DI constitutes relative to all sequenced DIs. **m**, As in **k**, but for GADD45A DIs. **n**, As in **l**, but for GADD45A DIs. Results are representative of two independently performed experiments.

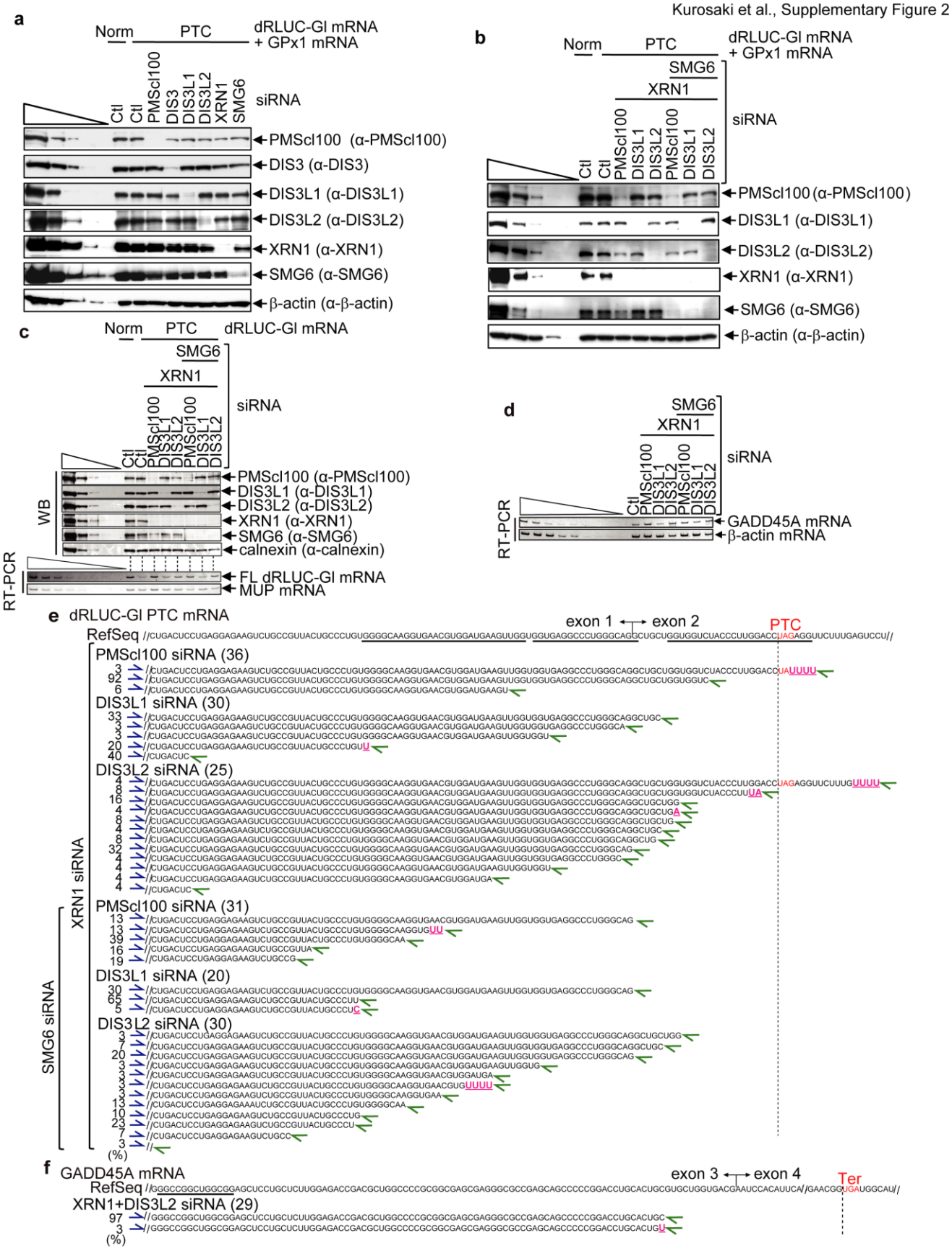
a
Norm
PTC
dRLUC-Gl mRNA
+ GPx1 mRNA
Ctl
Ctl
PMScl100
DIS3
DIS3L1
DIS3L2
XRN1
SMG6
siRNA
PMScl100 (α-PMScl100)
DIS3 (α-DIS3)
DIS3L1 (α-DIS3L1)
DIS3L2 (α-DIS3L2)
XRN1 (α-XRN1)
SMG6 (α-SMG6)
β-actin (α-β-actin)
b
Norm
PTC
dRLUC-Gl mRNA
+ GPx1 mRNA
SMG6
XRN1
siRNA
Ctl
Ctl
PMScl100
DIS3L1
DIS3L2
PMScl100
DIS3L1
DIS3L2
PMScl100 (α-PMScl100)
DIS3L1 (α-DIS3L1)
DIS3L2 (α-DIS3L2)
XRN1 (α-XRN1)
SMG6 (α-SMG6)
β-actin (α-β-actin)
c
Norm
PTC
dRLUC-Gl mRNA
SMG6
XRN1
siRNA
Ctl
Ctl
PMScl100
DIS3L1
DIS3L2
PMScl100
DIS3L1
DIS3L2
WB
PMScl100 (α-PMScl100)
DIS3L1 (α-DIS3L1)
DIS3L2 (α-DIS3L2)
XRN1 (α-XRN1)
SMG6 (α-SMG6)
calnexin (α-calnexin)
RT-PCR
FL dRLUC-Gl mRNA
MUP mRNA
d
SMG6
XRN1
siRNA
Ctl
PMScl100
DIS3L1
DIS3L2
PMScl100
DIS3L1
DIS3L2
RT-PCR
GADD45A mRNA
β-actin mRNA
e
dRLUC-Gl PTC mRNA
exon 1
exon 2
PTC
RefSeq
PMScl100 siRNA (36)
DIS3L1 siRNA (30)
DIS3L2 siRNA (25)
XRN1 siRNA
PMScl100 siRNA (31)
DIS3L1 siRNA (20)
DIS3L2 siRNA (30)
SMG6 siRNA
(%)
f
GADD45A mRNA
exon 3
exon 4
Ter
RefSeq
XRN1+DIS3L2 siRNA (29)
(%)

Supplementary Figure 2

Defining degradative activities that generate NMD DIs.

a, Western blotting of the samples analyzed in Fig. 2c,d. The five leftmost lanes represent threefold serial dilutions of lysate. Norm, normal; PTC, premature termination codon; Ctl, control. **b**, As in **a**, using multiple siRNAs where indicated. **c**, Western blotting (WB), SYBR-Gold-stained RT–PCR products of full-length (FL) dRLUC-Gl or MUP mRNA. **d**, As in **c**, but RT–PCR products of full-length GADD45A NMD target and β-actin mRNA. **e**, Sequences of dRLUC-Gl PTC decay intermediates (DIs) obtained in HEK293T cells transfected with the specified siRNAs. The PTC (red), exon 1–exon 2 junction, and putative G-quadruplex-forming sequences (underlined) are shown in the reference sequence (RefSeq). PCR primers (sense, blue arrows; antisense, green arrows) and nontemplated nucleotide additions (pink) are provided in the DIs, for which numbers in parentheses specify the number of clones sequenced and numbers to the left of the blue arrows denote the percent (%) that each DI constitutes relative to all sequenced DIs. **f**, Essentially as in **e** but for endogenous GADD45A mRNA. Ter (red) specifies the normal termination codon. Short sequencing products (<10 nt) were excluded from the analysis. NMD-DegNAs results are representative of two independently performed experiments.

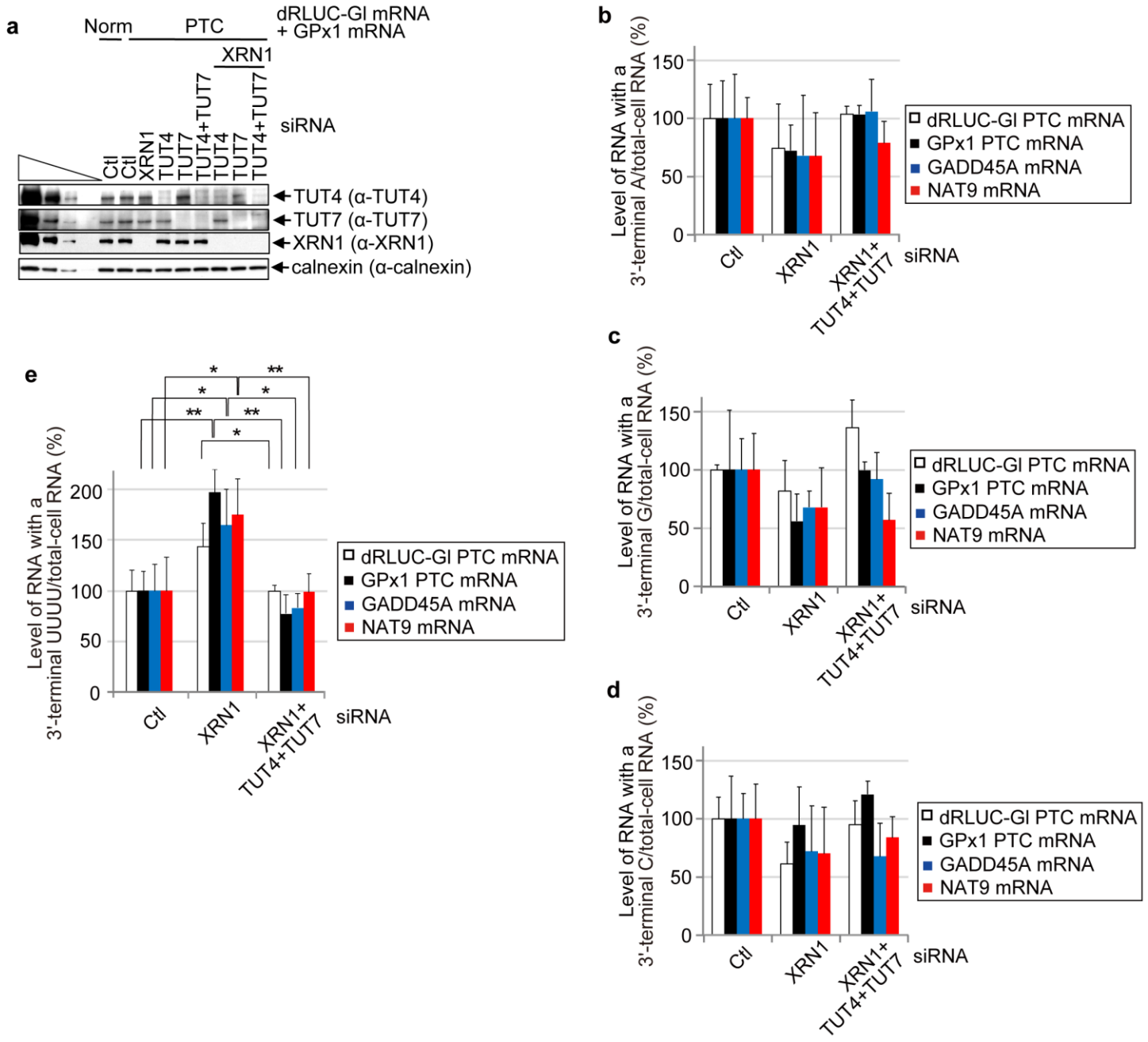

Supplementary Figure 3

NMD-target degradation involves terminal uridylyl transferases.

a, Western blotting of the HEK293T cell lysates analyzed in Fig. 3a–d**.** The four leftmost lanes represent threefold serial dilutions of lysate. Ctl, control. **b**, As in Fig. 3d, but for analyzing RNAs with 3'-terminal A after normalization to their level in total-cell RNAs. **c**, As in **b**, but for analyzing RNAs with 3'-terminal G. **d**, As in **b**, but for analyzing RNAs with 3'-terminal C. **e**, As in Fig. 3d, but analyzing RNAs ending with UUUU. *P < 0.05 and **P < 0.01 pertain to comparisons to Ctl siRNA or XRN1 siRNA samples (unpaired two-tailed t test); n = 3–4, showing means with s.d.

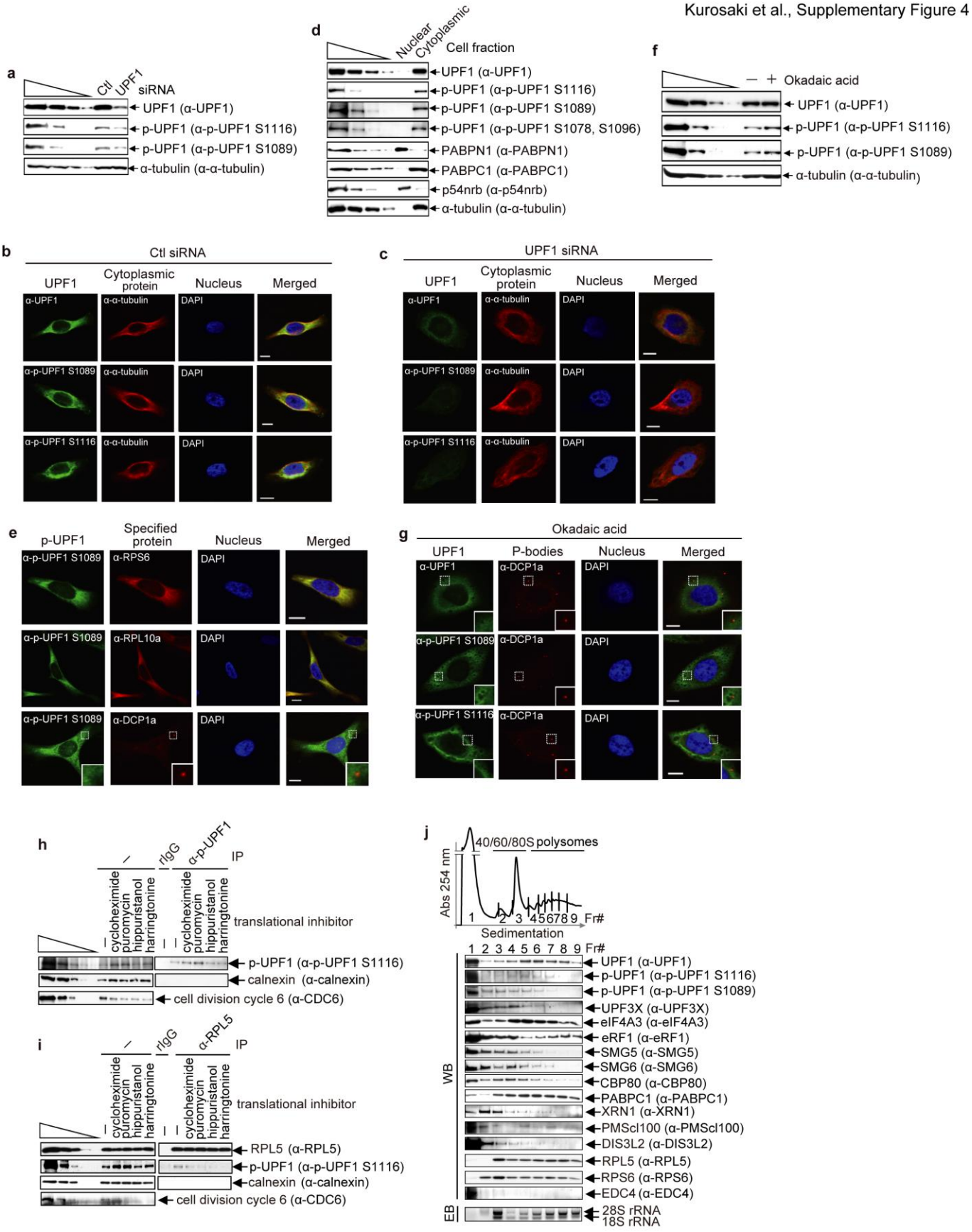
a
Ctl
UPF1
siRNA
UPF1 (α-UPF1)
p-UPF1 (α-p-UPF1 S1116)
p-UPF1 (α-p-UPF1 S1089)
α-tubulin (α-α-tubulin)
d
Nuclear
Cytoplasmic
Cell fraction
UPF1 (α-UPF1)
p-UPF1 (α-p-UPF1 S1116)
p-UPF1 (α-p-UPF1 S1089)
p-UPF1 (α-p-UPF1 S1078, S1096)
PABPN1 (α-PABPN1)
PABPC1 (α-PABPC1)
p54nrb (α-p54nrb)
α-tubulin (α-α-tubulin)
f
– + Okadaic acid
UPF1 (α-UPF1)
p-UPF1 (α-p-UPF1 S1116)
p-UPF1 (α-p-UPF1 S1089)
α-tubulin (α-α-tubulin)
b
Ctl siRNA
UPF1
Cytoplasmic protein
Nucleus
Merged
α-UPF1
α-α-tubulin
DAPI
α-p-UPF1 S1089
α-p-UPF1 S1116
c
UPF1 siRNA
e
p-UPF1
Specified protein
α-RPS6
α-RPL10a
α-DCP1a
g
Okadaic acid
P-bodies
h
–
rIgG
α-p-UPF1
IP
cycloheximide
puromycin
hippuristanol
harringtonine
translational inhibitor
p-UPF1 (α-p-UPF1 S1116)
calnexin (α-calnexin)
cell division cycle 6 (α-CDC6)
i
α-RPL5
RPL5 (α-RPL5)
j
40/60/80S polysomes
Abs 254 nm
Sedimentation
Fr#
WB
UPF3X (α-UPF3X)
eIF4A3 (α-eIF4A3)
eRF1 (α-eRF1)
SMG5 (α-SMG5)
SMG6 (α-SMG6)
CBP80 (α-CBP80)
PABPC1 (α-PABPC1)
XRN1 (α-XRN1)
PMScl100 (α-PMScl100)
DIS3L2 (α-DIS3L2)
RPS6 (α-RPS6)
EDC4 (α-EDC4)
EB
28S rRNA
18S rRNA

Supplementary Figure 4

p-UPF1 localizes diffusely throughout cytoplasm with ribosomal proteins and other NMD factors, and fails to co-immunoprecipitate with RPL5 when translation is inhibited.

a, Western blotting of lysates of HeLa cells (5×10^6/100-mm dish) transiently transfected with the specified siRNA. Ctl, control. **b**, Immunofluorescence microscopy of Ctl siRNA-treated HeLa cells (5×10^4/well of a 24-well plate) to localize anti(α)-UPF1, anti-p-UPF1(S1089) or anti-p-UPF1(S1116) reactivity, shown in green, relative to anti-α-tubulin reactivity, shown in red, and nuclei, stained blue using DAPI. Scale bar, 10 μm. **c**, As in **b** but using UPF1 siRNA-treated cells. **d**, Western blotting of nuclear and cytoplasmic fractions of HEK293T cells (8×10^7/150-mm dish). **e**, As in Fig. 4a, but using the specified antibody. **f**, Western blotting of lysates of HeLa cells (5×10^6/100-mm dish) that were or were not (−) exposed to 200 nM of okadaic acid for 3 h. **g**, Immunofluorescence microscopy of okadaic acid–treated HeLa cells (5×10^4/well using a 24-well plate) to localize anti(α)-UPF1, anti-p-UPF1(S1089) or anti-p-UPF1(S1116) reactivity, shown in green, relative to anti-Dcp1a reactivity, shown in red. Nuclei were stained blue using DAPI. Solid boxed regions are threefold magnifications of the dotted boxed regions. Scale bar, 10 μm. **h**, Western blotting of the samples assayed in Fig. 4b. Translation inhibition was evaluated by measuring the abundance of cell division cycle 6 (CDC6) protein, which has a half-life of 2–4 h (*Genes Dev*. **14**, 2330–2343, 2000; *Eur. J. Biochem*. **269**, 1040–1046, 2002). **i**, As in **h**, but IP used anti(α)-RPL5. **j**, Using fractions from polysome profile of HEK293T cell lysates shown (top), western blotting (WB) using the specified antibody and ethidium bromide staining (EB) to analyze 28S and 18S rRNAs.

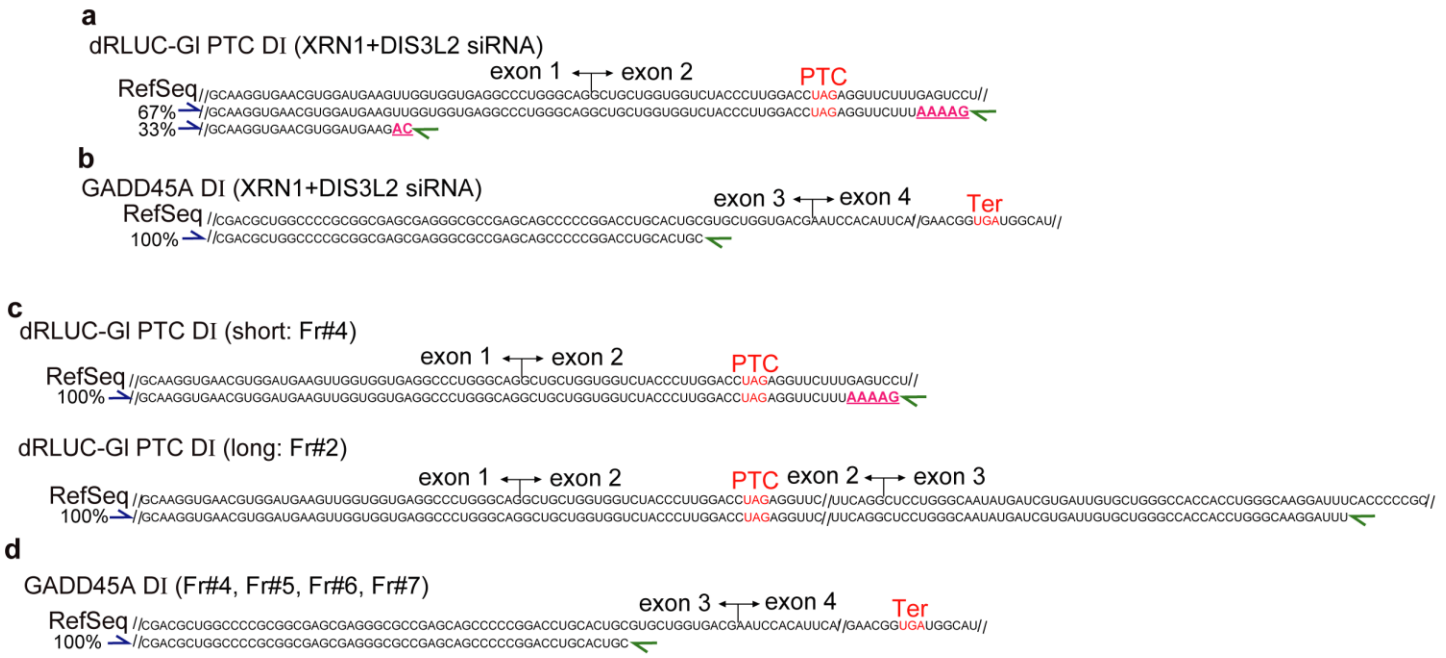

Supplementary Figure 5

Sequences of NMD DIs from NMD-DegRPL5 and NMD-DegRibo.

a, Sequences of the dRLUC-GI PTC DIs obtained in Fig. 5c. The PTC (red) and exon 1–exon 2 junction are shown in the reference sequence (RefSeq). PCR primers (sense, blue arrows; antisense, green arrows) and nontemplated nucleotide additions (pink) are provided in the DIs, for which numbers to the left of the blue arrows denote the percent (%) that each DI constitutes relative to all sequenced DIs. **b**, As in **a**, but for the GADD45A DIs obtained in Fig. 5d. Ter (red) specifies the normal termination codon. **c**, dRLUC-GI PTC DIs were obtained in Fig. 5f. RNA samples were generated using the scheme outlined for polysome fractionation shown in Fig. 5a. **d.** As in c, but for the GADD45A NMD target DIs obtained in Fig. 5g.

Supplementary information

NMD-degradome sequencing reveals ribosome-bound intermediates with 3'-end nontemplated nucleotides

Tatsuaki Kurosaki [1,2], Keita Miyoshi [1,2,4], Jason R. Myers[3] and Lynne E. Maquat [1,2,*]

[1]Department of Biochemistry and Biophysics, School of Medicine and Dentistry, University of Rochester, Rochester, New York 14642, USA
[2]Center for RNA Biology, University of Rochester, Rochester, New York 14642, USA
[3]Genomics Research Center, University of Rochester, Rochester, New York 14642, USA

[4]Present Address: Division of Invertebrate Genetics, National Institute of Genetics, 1111 Yata, Mishima, Shizuoka 411-8540, Japan

*e-mail: lynne_maquat@urmc.rochester.edu

Supplementary Notes

Supplementary Note 1 | Streamlined NMD-DegSeq confirms the addition of nontemplated nucleotides to NMD DIs. Transcriptome-wide NMD-DegSeq indicates that the 3'-ends of many NMD decay intermediates (DIs) have been "tailed" with one or more nontemplated nucleotides. To corroborate these findings, we developed a streamlined version of NMD-DegSeq and included assays of NMD reporter transcripts.

HEK293T cells were transiently co-transfected with two reporter plasmids and one reference plasmid. Reporter plasmids encode dRLUC-Gl mRNA or GPx1 mRNA, each either nonsense-free (Norm) or harboring an NMD-triggering premature termination codon (PTC) that derive, respectively, from a deletion-bearing (d) Renilla luciferase (RLUC) gene fused to a β-

globin (Gl) gene or a glutathione peroxidase 1 (GPx1) gene; the reference plasmid encodes mouse major urinary protein (MUP) mRNA[6,30,44]. After 2 days, cells were treated with 200 nM of okadaic acid for 3 hr and then lysed. Cell lysates were immunoprecipitated using anti-p-UPF1 or rIgG (Supplementary Fig. **1i**, **j**), cDNA was synthesized by priming a 20-nt RNA adapter that was ligated to RNA 3'-ends, cDNAs were PCR-amplified using a sense primer to individual mRNAs of interest and the same antisense primer used to generate cDNA, PCR products were TA-cloned into plasmid DNA, and individual DNA clones were sequenced (Supplementary Fig. **1i**).

Remarkably, only a single or two PCR products were evident for, respectively, p-UPF1-bound dRLUC-Gl PTC mRNA (Supplementary Fig. **1k, l**) and p-UPF1-bound cellular mRNA encoding growth arrest and DNA damage inducible A (GADD45A) (Supplementary Fig. **1m, n**), which is an endogenous NMD target in HEK293T cells since the normal termination codon (Ter) triggers NMD[6,10,37,39]. DNA sequencing PCR products deriving from p-UPF1-bound dRLUC-Gl PTC DIs revealed that all 15 clones had the same five nontemplated nucleotides, AAAAG, added 9-nucleotides downstream of the PTC (Supplementary Fig. **1l**). Of the two DIs deriving from p-UPF1-bound GADD45A mRNA, the shorter had 3'-ends ending 123 nucleotides upstream of Ter, the longer had 3'-ends ending 99 nucleotides downstream of Ter, and none appeared to have tailed 3'-ends (Supplementary Fig. **1n**).

Supplementary Note 2 | NMD-DegNA demonstrates that NMD is largely mediated by nucleases acting at mRNA 5'- and 3'-ends. RT-qPCR revealed that (i) the level of each PTC-containing NMD reporter mRNA or cellular NMD target was not significantly upregulated by siRNA to either exosomal 3'-to-5' exonuclease DIS3 or DIS3L1, (ii) both reporter mRNAs were

significantly upregulated by siRNA to the exosome-free 3'-to-5' exonuclease DIS3L2, but only dRLUC-Gl reporter mRNA was significantly upregulated by siRNA to the exosomal 3'-to-5' exonuclease PMScl100 as well as the 5'-to-3' exonuclease XRN1, and (iii) the GADD45A cellular NMD target was upregulated by PMScl100 siRNA (Fig. **2c**, **d**). Additionally, for NMD reporter mRNAs, downregulating either PMScl100 or DIS3L2 and, in the case of both cellular NMD targets, downregulating PMScl100 or SMG6 tended to increase XRN1 siRNA-mediated effects (Fig. **2c**, **d**). In control experiments, no single siRNA or combination of siRNAs that was assayed significantly upregulated the level of dRLUC-Gl Norm mRNA, GPx1 Norm mRNA, or cellular GAPDH mRNA (data not shown).

We conclude for HEK293T cells that while the decay of the tested NMD targets is largely mediated by nucleases acting at mRNA 5'- and 3'-ends, the degree to which each target is upregulated by the downregulation of individual or combinations of decay factors can vary. Our finding that NMD can involve the addition of nontemplated nucleotides to DI 3'-ends (Fig. **1** and Supplementary Fig. **1**) is consistent with the sensitivity of NMD targets to the processive 3'-to-5' hydrolytic exoribonuclease DIS3L2, which preferentially degrades RNAs with modified 3'-ends (U_{15}> C_{15}>> A_{15}), where 12 Us constitute a DIS3L2 recognition signal[25]. Our finding that NMD DIs harbor fewer than 12 nontemplated Us (Fig. **1g**) indicates that further 3'-to-5' exonucleolytic decay must be rate-limiting.

Supplementary Note 3 | Resolving the controversy over whether p-UPF1 resides at translationally active cellular sites. While a number of publications have argued for NMD occurring in processing bodies (P-bodies), i.e. in a ribosome-free state[72-74] or, as recently as last summer, another type of cytoplasmic body[75], the possibility that the decay steps of NMD take

place during mRNA translation in a ribosome-bound state remains debatable[32,76,77]. Certainly, steps preceding the mRNA decay steps of NMD involve translationally active mRNA. For example, PTC recognition during NMD occurs while an NMD target is bound by translationally active ribosomes since reinitiation downstream of a PTC but upstream of an EJC inhibits NMD[78,79]. Additionally, UPF1 phosphorylation, which is triggered by PTC recognition, also occurs on an NMD target bound by translationally active ribosomes given that decay requires the p-UPF1-mediated inhibition of 60S ribosome subunit joining to a 43S pre-initiation complex poised at the translation initiation codon of the targeted mRNA, indicating that the mRNA is in the process of translation re-initiation[36].

In support of the decay steps of NMD occurring in ribosome-free P-bodies, mRNA-decapping enzyme (DCP)2 and its binding partner DCP1 as well as NMD factors SMG5 and SMG7, which are recruited to NMD targets by p-UPF1[6,14,15,35], are enriched in P-bodies in mammalian cells[31-33,54,55], where some data suggest that translationally repressed PTC-containing mRNPs undergo decapping[72]. Moreover, PNRC2, which preferentially interacts with p-UPF1 together with SMG5 and DCP1a, has been reported to recruit UPF1 to P-bodies[31,33]. Additionally, exogenously expressed ATPase-deficient UPF1 variants, which unlike wild-type UPF1 are trapped in a phosphorylated state, localize predominantly to P-bodies[31-33,77], suggesting that the initiation of NMD decay occurs in P-bodies. Nevertheless, several lines of evidence show that blocking detectable P-body formation in human cells does not inhibit NMD, indicating that P-body formation *per se* is not required for mRNA decay[76,77].

Our finding using IF that cellular p-UPF1 is not enriched in ribosome-free cytoplasmic P-bodies, as is the DCP1a P-body protein, but instead resides throughout the cell cytoplasm, as do small and large ribosome subunit proteins (Fig. **4** and Supplementary Fig. **4**), contrasts reports

that exogenously expressed p-UPF1 variants that are ATPase-helicase deficient localize to P-bodies[31-33,77]. This localization to P-bodies could reflect their ATPase-helicase deficiency; it could additionally or alternatively reflect that p-UFP1 variants, NMD reporter transcripts, or some combination thereof were experimentally engineered to be over-expressed. Regarding the first point, UPF1 variants are not apt to be suitable markers of NMD targets and, thus, appropriate indicators of the cellular site of NMD. For example, one of the variants assayed, MYC-UPF1(G495R, G497E), manifests a high degree of nonspecific binding to cellular RNAs because ATP cleavage is required to release of UPF1 from RNA binding, without which UPF1 becomes hyperphosphorylated[6,80]. Moreover, other variants tested, i.e. MYC-UPF1(G495R, G497E), MYC-UPF1 (D636A, E637A) or MYC-UPF1(K498A), fail to support NMD[32,36].

Supplementary Note 4 | p-UPF1 is ribosome-bound along with other NMD factors. Western blots of polysome fractions revealed that p-UPF1 exists in ribosome-free and ribosome-bound fractions (respectively, Fr#1 and Fr#2-7 in Supplementary Fig. **4j**) with other NMD factors. In contrast, the P-body marker EDC4[32,76,77] is restricted to the ribosome-free fraction. Our finding that NMD DIs are detected in association with ribosomes (Fr#4-7 in Fig. **5f**, **g**) indicates that p-UPF1 in the ribosome-free fraction is not largely active in generating NMD DIs, but rather may be in the process of recycling to a hypo-phosphorylated form by protein phosphatase 2A[6].

Supplementary Note 5 | Supplementary Discussion

While it was previously shown that downregulating exosome constituents stabilizes NMD reporters[12,46], the nature of the resulting DIs was ambiguous[9,17,32]. We report here that DIS3L2, the PMScl100 exosome constituent, and the TUT4 and TUT7 terminal uridylyl transferases are

among the RNA activities that generate NMD DIs (Fig. **2**, **3**, **5** and Supplementary Fig. **2**, **3**). Moreover, these DIs in the steady-state generally contain fewer than 12 nontemplated uridines (Fig. **1f, g**). This number of uridines is a recognition signal for DIS3L2[25] and also attractive to the exosome given its need for an unstructured 3'-end[81]. Thus, the observed DIs likely derive from precursor DIs containing longer, i.e. ≥12, non-templated nucleotide additions that were appended by TUT4 and TUT7 and subsequently shortened by DIS3L2 (Fig. **2**, **3**, **5** and Supplementary Fig. **2**, **3**) or, to a lesser degree, the exosome (Fig. **2** and Supplementary Fig. **2**). In theory, the 3'-end Us may also recruit Lsm1-7 so as to promote both 5'-to-3' and 3'-to-5' exonucleolytic decay[82, 83](Fig. **6**), consistent with our observation that 3'-end decay cooperatively promotes 5'-end decay (Fig. **3** and Supplementary Fig. **3**).

Our detecting DIs containing an appended heterogeneous stretch of nontemplated nucleotides (Fig. **1, 2, 5** and Supplementary Fig. **1**) may implicate TUT4 and TUT7 function or the function of other TUTases such as TUT2, which has been shown to add not only U but also A, C or G[84]. Non-U additions have been observed previously in both mRNA transcribed regions and at the end of partially shortened poly(A) tails[23,26,43], although the responsible polymerase(s) were not defined. While it appears that human NMD has evolved to combine multiple processes to accelerate mRNA degradation, initiated by a series of carefully choreographed steps that involve translation termination of the type that evokes UPF1 activation by phosphorylation, aside from the specialized function of the SMG6 endonuclease, NMD DIs with nontemplated U additions appear to be generated as are those DIs typifying general mRNA decay, histone mRNA decay, pre-miRNA decay and long-noncoding RNA decay[22-29,43,53,85].

It is remarkable that the DI deriving from dRLUC-Gl PTC mRNA, whose 3'-end is situated 9-nucleotides downstream of the PTC and invariably appended with nontemplated

AAAAG, is found in IPs of p-UPF1 (Supplementary Fig. **1k**, **l**) and RPL5 (Fig. **5c** and Supplementary Fig. **5a**) as well as on polysomes after downregulating XRN1 and DIS3L2 (Fig. **5f** and Supplementary Fig. **5c**). SMG6 favors cleaving Gl PTC mRNA in the proximity of the PTC[9-11]. Since this DI is not evident after downregulating XRN1 and PMScl100 either with or without an appended AAAAG (Fig. **5c**), it is likely that its derivation involves DIS3L2 activity and that this activity may be stalled, much as how histone mRNAs undergo a series of oligouridylations, each occurring upstream of the previous as required for 3'-to-5' decay at the end of S phase of the cell cycle, also on polysomes[49,51]. SMG6 influences the nature of dRLUC-Gl PTC DI 3'-ends (Fig. **2f** and Supplementary Fig. **2e**), consistent with reports of SMG6 function during the NMD of Gl PTC mRNA[6,9,10]. As during general mRNA decay[26,29,43], the cellular abundance of short nontemplated appendages of one or a few nucleotides that we detect at the 3'-ends of DIs are expected to be more stable than their precursor DIs, which would have had longer appendages, in view that the length of added Us negatively correlates with RNA stability[43]. Also, putative G-quadruplex structures are enriched upstream of dRLUC-Gl NMD DI 3'-ends (Supplementary Fig. **2e**), suggesting that local RNA structures stall DIS3L2 or exosome progression.

We also observed one particular DI for the GADD45A NMD target in IPs of either p-UPF1 (Supplementary Fig. **1m, n**) or RPL5 (Fig. **5d** and Supplementary Fig. **5b**) as well as on polysomes after downregulating XRN1 and DIS3L2 (Fig. **5g** and Supplementary Fig. **5d**). Since the 3'-end of this DI is situated 123-nucleotides upstream of the termination codon that triggers NMD, i.e. the normal termination codon, it is unlikely that it is generated directly by SMG6, but it appears to be a template for either DIS3L2 or PMScl100 decay and may also be the consequence of a block in their processivity.

Supplementary references

72. Cougot, N., Babajko, S. & Séraphin, B. Cytoplasmic foci are sites of mRNA decay in human cells. *J. Cell Biol*. **165**, 31–40 (2004).
73. Sheth, U. & Parker, R. Targeting of aberrant mRNAs to cytoplasmic processing bodies. *Cell* **125**, 1095–1109 (2006).
74. Durand, S. et al. Inhibition of nonsense-mediated mRNA decay (NMD) by a new chemical molecule reveals the dynamic of NMD factors in P-bodies. *J. Cell Biol.* **178**, 1145–1160 (2007).
75. Jia, J. et al. Premature termination codon readthrough in human cells occurs in novel cytoplasmic foci and requires UPF proteins. *J. Cell Sci.* **130**, 3009–3022 (2017).
76. Eulalio, A., Behm-Ansmant, I., Schweizer, D. & Izaurralde, E. P-body formation is a consequence, not the cause, of RNA-mediated gene silencing. *Mol. Cell. Biol*. **27**, 3970–3981 (2007).
77. Stalder, L. & Mühlemann, O. Processing bodies are not required for mammalian nonsense-mediated mRNA decay. *RNA* **15**, 1265–1273 (2009).
78. Zhang, J. & Maquat, L.E. Evidence that translation reinitiation abrogates nonsense-mediated mRNA decay in mammalian cells. *EMBO J*. **16**, 826–833 (1997).
79. Neu-Yilik, G. et al. Mechanism of escape from nonsense-mediated mRNA decay of human beta-globin transcripts with nonsense mutations in the first exon. *RNA* **5**, 843–854 (2011).
80. Lee, S. R., Pratt, G. A., Martinez, F. J., Yeo, G. W. & Lykke-Andersen, J. Target discrimination in nonsense-mediated mRNA decay requires Upf1 ATPase activity. *Mol. Cell* **59**, 413–425 (2015).
81. Zinder, J. C. & Lima, C.D. Targeting RNA for processing or destruction by the eukaryotic RNA exosome and its cofactors. *Genes Dev.* **31**, 88-100 (2017).
82. Lyons, S. M., Ricciardi, A. S., Guo, A. Y., Kambach, C. & Marzluff, W. F. The C-terminal extension of Lsm4 interacts directly with the 3′ end of the histone mRNP and is required for efficient histone mRNA degradation. *RNA* **20,** 88–102 (2014).
83. Norbury, C. J. Cytoplasmic RNA: a case of the tail wagging the dog. *Nat Rev Cancer* **13**, 643–653. (2013).
84. Heo, I. et al. Mono-uridylation of pre-microRNA as a key step in the biogenesis of group II let-7 microRNAs. *Cell* **151**, 521–532 (2012).
85. Su, W. et al. mRNAs containing the histone 3′ stem-loop are degraded primarily by decapping mediated by oligouridylation of the 3′ end. *RNA* **19**, 1–16 (2013).

Supplementary Table 2 | List of siRNA target sequences used in the specified figures.

Figure	siRNA	siRNA target sequence
Fig. **2**, **3**, **5**, Supplementary Fig. **2**, **3**	XRN1	5'-AGAUGAACUUACCGUAGAA-3'
Fig. **2**, Supplementary Fig. **2**	SMG6	5'-GGCUGAUUUCUGUAACAUA-3'
Fig. **2**, Supplementary Fig. **2**	PMScl100	5'-GCAGAGUAAUGCAGUACCA-3'
Fig. **2**, Supplementary Fig. **2**	DIS3	5'-AGGUAGAGUUGUAGGAAUA-3'
Fig. **2**, Supplementary Fig. **2**	DIS3L1	5'-CCAUGUAACCGUAAGAAUA-3'
Fig. **2**, Supplementary Fig. **2**	DIS3L2	5'-GUAGUUAAACCAGAGAGCA-3'
Fig. **3**, Supplementary Fig. **3**	TUT4	5'-GGAGAAACGACAUAAGAAA-3'
Fig. **3**, Supplementary Fig. **3**	TUT7	5'-GAUAAGUAUUCGUGUCAAA-3'
Supplementary Fig. **4**	UPF1	5'-GAUGCAGUUCCGCUCCAUU-3'

Supplementary Table 3 | List of primers used in NMD-DegSeq, RT, PCR or qPCR.

Name	Sequence(s)
3'-DNA adapter for NMD-DegSeq	5'-App-CTGTCTCTTATACACATCTCCGAGCCCACGAGAC-ddC-3'
5'-RNA adapter for NMD-DegSeq	5'-UCGUCGGCAGCGUCAGAUGUGUAUAAGAGACAG-3'
1st strand RT for NMD-DegSeq	5'-GTCTCGTGGGCTCGGAGATGTGTATAAGAGACAG-3'
1st PCR sense for NMD-DegSeq	5'-TCGTCGGCAGCGTCAG-3'
1st PCR antisense for NMD-DegSeq	5'-GTCTCGTGGGCTCGGA-3'
dRLUC-Gl mRNA sense	5'-TCTGCCGTTACTGCCCTGTG-3'
dRLUC-Gl mRNA antisense	5'-GGGTTTAGTGGTACTTGTGAGC-3'
GPx1 mRNA sense	5'-ACCACCGTAGAACGCAGATCG-3'
GPx1 mRNA antisense	5'-AATCTCTTCATTCTTGCCATTCTC-3'
MUP mRNA sense	5'-CTGATGGGGCTCTATG-3'
MUP mRNA antisense	5'-TCCTGGTGAGAAGTCTCC-3'
GADD45A mRNA sense	5'-GGAGGAATTCTCGGCTGGAG-3'
GADD45A mRNA antisense	5'-CGTTATCGGGGTCGACGTT-3'
GADD45A pre-mRNA sense	5'-TTGCAGGGAACCCAACTACC-3'
GADD45A pre-mRNA antisense	5'-TCCTTCCATTGAGATGAATGTGG-3'
NAT9 mRNA sense	5'-GGTCCTTGTACCCTACACCTC-3'
NAT9 mRNA antisense	5'-CTGCACTGCATGGCATACT-3'
NAT9 pre-mRNA sense	5'-CCTGTCTCATCTCCTCTG-3'
NAT9 pre-mRNA antisense	5'-TCCTTACCTGCTCAAAGT-3'
3'-RNA adapter	5'-p-GUACUAGUCGACGCGUGGCC-ddC-3'
Adapter antisense	5'-GGCCACGCGTCGACTAGTAC-3'
CMV promoter sense	5'-ACCACCGTAGAACGCAGATCG-3'
dRLUC-Gl FL mRNA antisense	5'-CACGATCATATTGCCCAGGAG-3'
2nd PCR dRLUC-Gl DI sense	5'-TGGAGCGCGTGCTGAAGAAC-3'
2nd PCR GADD45A DI sense	5'-GAGCTCCTGCTCTTGGAGAC-3'
β-actin mRNA sense	5'-AATCGTGCGTGACATTAAG-3'
β-actin mRNA antisense	5'-ATGATGGAGTTGAAGGTAGT-3'
Adapter antisense for a 3′-terminal U	5'-GGCCACGCGTCGACTAGTACA-3'
Adapter antisense for a 3′-terminal A	5'-GGCCACGCGTCGACTAGTACT-3'
Adapter antisense for a 3′-terminal G	5'-GGCCACGCGTCGACTAGTACC-3'
Adapter antisense for a 3′-terminal C	5'-GGCCACGCGTCGACTAGTACG-3'
Adapter antisense for a 3′-terminal UUUU	5'-GGCCACGCGTCGACTAGTACAAAA-3'
GADD45B mRNA sense	5'-TTGTCTCCTGGTCACGAACC-3'
GADD45B mRNA antisense	5'-TGTGGCAGCAACTCAACAGA-3'
TRAF2 mRNA sense	5'-GCTCATGCTGACCGAATGTC-3'
TRAF2 mRNA antisense	5'-GCCGTCACAAGTTAAGGGGAA-3'
SMG5 mRNA sense	5'-AGATGGCATGTCACCGATGTC-3'
SMG5 mRNA antisense	5'-GGGCTTGGTAGTAAAATCTCTCG-3'
GAPDH mRNA sense	5'-GTCGCCAGCCGAGCCACATC-3'
GAPDH mRNA antisense	5'-CCAGGCGCCCAATACGACCA-3'
18S rRNA sense	5'-GGGAAACCAAAGTCTTTGGG-3'
18S rRNA antisense	5'-GGAATTAACCAGACAAATCGC-3'